Polarization Frederiks-Transition in SmC* Liquid Crystal Films

W. Zimmermann,[1] S. Ried,[2,3] H. Pleiner,[3] and H.R. Brand[4]

[1] *Forschungszentrum Jülich, IFF, D 52425 Jülich, Germany*
[2] *Universität Essen, FB 7, Physik, D 45117 Essen, Germany*
[3] *Max-Planck-Institut für Polymerforschung, D 55021 Mainz, Germany*
[4] *Theoretische Physik III, Universität Bayreuth, D 95440 Bayreuth, Germany*

October 13, 2008

I. Introduction

The generalized Frederiks transition in freely suspended smectic C* films is theoretically investigated and put in relation to the electroconvection presented a year ago [1]. In the past the Frederiks transition in nematics has always been considered to be continuous. But the inclusion of an additional ferroelectric torque leads to rather complicated bifurcation scenarios even in the case of DC Frederiks transitions. There are two different instability branches and a restabilization curve [2].

Depending on material parameters these transitions switch from being continuous to discontinuous. If the polarization is large enough and antiparallel to the external field, a Frederiks transition is possible even for negative dielectric anisotropy. In a certain parameter range the restabilization of the homogeneous state is not obtained, since the latter exists as an isolated solution, only.

A model system is introduced to produce analytic amplitude equations for any bifurcation scenario with two branches and restabilization.

II. Basic Equations and Geometry

This work is focused on a liquid crystal film of a smectic phase. This phase is organized in layers, where in the smectic C phase (SmC) the director $\boldsymbol{n}$ is tilted by a fixed angle ψ relative to the layer normal $\boldsymbol{k}$. The projection of $\boldsymbol{n}$ onto the plane of the smectic layers is the $\boldsymbol{c}$ director, which can be observed by polarized light normal to the layer. Due to the existence of $\boldsymbol{k}$ and $\boldsymbol{c}$ this phase is biaxial.

The chiral smectic C* phase (SmC*) shows in addition an intrinsic twist of the director from layer to layer. This additional symmetry breaking ($C_{2h} \to C_2$ locally) allows microscopic electric dipoles to form a spontaneous electric polarization $\boldsymbol{P}$, which lies in the smectic planes (perpendicular to both $\boldsymbol{k}$ and $\boldsymbol{c}$) and is twisted, too. We will neglect this twist in the following thus assuming that the thickness of the freely suspended film is small compared to the pitch of the helielectric C* phase [3], which is typically $\sim 1 \ldots 10\,\mu m$.

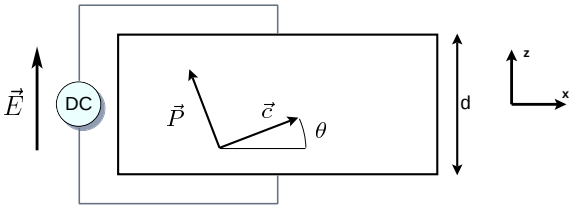

Fig.1 *One layer of SmC* is shown from above. The electric field is applied along the z-direction. The length of the film (in x-direction) is assumed to be much longer than its width d. The layer normal* $\mathbf{k}$ *is perpendicular to the plane of drawing.*

The considered experimental setup is shown in Fig. 1 (cf. Ref.[1] and Ref.[4]) and is just similar to recent experiments giving hints to electroconvection in SmC* films [5].

We derive first the fully nonlinear equations to investigate director deformations above a DC-driven splay Frederiks-transition, which are assumed to be homogeneous in x-direction. A linearized form is used in chapter (III). The backflow is very weak in this situation [6] and will be neglected. With notation and scalings of [2] we write down the energy density f_G containing a dielectric part f_E and an elastic part f_F:

$$f_G = f_F + f_e \tag{1}$$

$$f_e = -\frac{1}{2}\epsilon_{ij}E_iE_j - P_iE_i \tag{2}$$

$$f_F = \frac{1}{2}F_{22}(\mathrm{div}\,\boldsymbol{c})^2 + \frac{1}{2}F_{33}(\boldsymbol{c}\cdot\mathrm{curl}\,\boldsymbol{c})^2 + \frac{1}{2}F_{11}(\boldsymbol{c}\times\mathrm{curl}\,\boldsymbol{c})^2\,, \tag{3}$$

Where the anisotropic tensors are of the form $\epsilon_{ij} = \epsilon_\perp\delta_{ij} + \epsilon_a c_i c_j$ and $\epsilon_\perp$ is the dielectric constant perpendicular to the director $\boldsymbol{c}$. F_{22} is the splay, F_{33} the twist and F_{11} the bend elastic constant introduced first in [7]. The molecular field h_i and the dielectric displacement D_i are given by

$$h_i = -\frac{\delta f_G}{\delta c_i} \qquad D_i = -\frac{\delta f_G}{\delta E_i} \tag{4}$$

where the electric field E_i is due to the applied voltage V as well as due to the induced potential. In the given geometry only two degrees of freedom are left, one angle $\theta(z,t)$ of the director orientation and the induced electric potential $\phi(z,t)$. The nonlinear balance equation of the director is given by

$$\partial_t c_i = \frac{1}{\gamma_1}\delta^{tr}_{ik} h_k \tag{5}$$

where $\delta^{tr}_{ik} = \delta_{ik} - c_i c_k$. With $c_z = \sin\theta$ this takes the (dimensionless) form:

$$\begin{aligned}\partial_t\theta &= \left((1-c_3^2)h_z - c_x c_z h_x\right)/\cos\theta \\ &= \left(\frac{F_{11}}{F_{22}}\sin^2\theta + \cos^2\theta\right)\partial_z^2\theta \\ &\quad + \Bigg(\left(\frac{F_{11}}{F_{22}} - 1\right)(\partial_z\theta)^2 \\ &\quad + \frac{\epsilon_a}{\epsilon_\perp}(V(t) - \partial_z\phi(z,t))^2\Bigg)\sin\theta\cos\theta \\ &\quad - \sin\theta\; p_0\;\; (V(t) - \partial_z\phi(z,t))\end{aligned} \tag{6}$$

The equation of motion for ϕ is derived from the Maxwell equation $\mathrm{div}\boldsymbol{D} = \rho$. Eliminating ρ via the electric current density $j^e_i = \sigma_{ij}E_j$ and the charge conservation $\partial_t\,\rho + \boldsymbol{\nabla}\cdot\boldsymbol{j}^e = 0$ one gets

$$0 = \partial_t\left(\boldsymbol{\nabla}\cdot\boldsymbol{D}\right) + \boldsymbol{\nabla}\cdot\boldsymbol{j}^e\,. \tag{7}$$

Equations (6) and (7) describe so far the full nonlinear dynamics of the problem. Since Eq.(7) gets rather complicated we expand it for the static case $\partial_t\phi = 0$ only and get

$$\begin{aligned}0 &= 2\frac{\sigma_a}{\sigma_\perp}\sin\theta\cos\theta\,(V - \partial_z\phi(z))\;\partial_z\theta \\ &\quad - \left(1 + \frac{\sigma_a}{\sigma_\perp}\sin^2\theta\right)\partial_z^2\phi \quad .\end{aligned} \tag{8}$$

III. Linear Stability

Threshold values for applied DC voltages at which the Frederiks transition occurs are calculated from the linear parts of Eqs.(6) and (8) for deviations θ and ϕ from the planar ground state ($\theta_g = 0$, $\phi_g = 0$). In that limit these equations are decoupled and the trivial solution $\theta = \theta_g = 0$ is obtained for the induced potential. Eq.(6) is solved by the ansatz $\theta(t,z) = e^{\lambda t}A_0\cos z$. Thus the basic state becomes unstable for positive growth rates λ of θ and the threshold is defined by the condition $\lambda = 0$.

For non-zero values of p_0 and ε_a, there are two orientational torques. One is due to the dielectric anisotropy, ε_a and the other is the ferroelectric torque due to the spontaneous polarization. The threshold formula of this generalized Frederiks instability due to the applied DC voltage is given by [2]

$$p_0 V_{c\,1,2} = \frac{1}{2F}\left[1 \pm \sqrt{1+4F}\right] \tag{9}$$

with

$$F \equiv \frac{\varepsilon_a}{\varepsilon_\perp p_0^2}\,. \tag{10}$$

This formula contains both, the traditional splay Frederiks effect (due to dielectric torques) and the pure "polarization Frederiks effect" (due to ferroelectric torques). Since polarization and director are rigidly coupled, both effects can either enhance each other (for $p_0V < 0$, i.e. for an external field antiparallel to the polarization, and for $F > 0$, i.e. for positive dielectric anisotropy $\varepsilon_a > 0$) and therefore reduce the threshold voltage, or they counteract each other (for $p_0V > 0$ and $F > 0$) increasing the threshold voltage (cf. Fig. 2). In the limit $F \to +\infty$ (vanishing polarization and positive dielectric anisotropy) the two instability lines coalesce restoring the degeneracy due to the $\pm V$ symmetry in this limit.

In contrast to the traditional splay Frederiks transition that exists only for $\varepsilon_a > 0$, the general Frederiks transition can exist even for negative dielectric anisotropy (for $p_0V < 0$), if p_0 exceeds a critical value $p_0 > p_c$ with

$$p_c = \sqrt{\frac{-4\varepsilon_a}{\varepsilon_\perp}}\;. \tag{11}$$

In that case the destabilizing effect due to the polarization overcomes the stabilizing effect due to the dielectric anisotropy. Thus in Fig.2 the solid line, below which the planar initial configuration is Frederiks-unstable, extends to $F < 0$, but ends at $F = -1/4$.

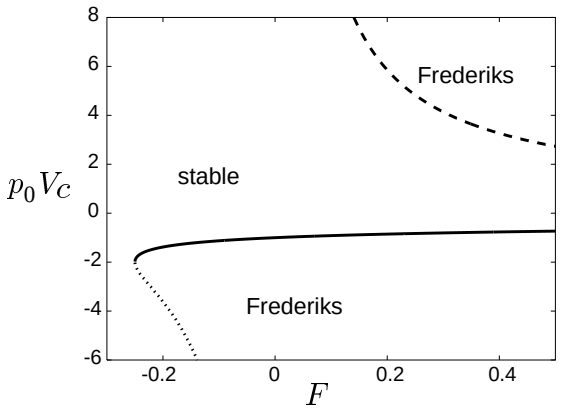

Fig.2 *The threshold for the general splay Frederiks transition is shown as function of the quantity* $F = \varepsilon_a/(\varepsilon_\perp p_0^2)$. *The dashed curve branches out of the traditional Frederiks transition and the solid line describes the new branch due to the polarization Frederiks effect, whereas the dotted line shows the linear restabilization of the basic state* $\theta_g = 0$.

This branch is new and owes its existence to the polarization Frederiks effect. However, since the destabilizing effect is linear in the external field strength while the stabilizing one is quadratic, the latter will win above a certain (higher) threshold, above which the ground state becomes stable again. This restabilization is shown as dotted curve in Fig.2. Since

the stabilizing effect vanishes for $\varepsilon_a \to 0_-$, the dotted curve diverges in this limit. On the other hand, if p_0 is too small ($p_0 < p_c$), the linear destabilizing effect is too weak to trigger the instability and the ground state is Frederiks stable.

IV. Nonlinear Regime

To get an overview of what could happen for large director deformations we have integrated the coupled system of Eqs.(6,8) numerically. As a characterization of the nonlinear director field the integrated director deformation is introduced

$$B = \frac{1}{2} \int_{-\pi/2}^{\pi/2} \theta(z)\, dz \tag{12}$$

and interpreted as an order parameter. B vanishes for the basic state ($\theta_g = 0$) and reduces to $B = A$ for small director deformations $\theta(z) = A \cos z$. Above the dashed threshold line in Fig.2 ($p_0 V_c > 0$ and $F > 0$) the bifurcation from the basic state is continuous and the dielectric torque dominates both, the ferroelectric and the elastic one. Thus, $\theta = \pi/2$ is favored as equilibrium state and for large voltages, $\eta \to \infty$, B approaches $\pi^2/4$ from below.

For the new instability branch (solid line in Fig.2) the bifurcation behavior is more complex. In the range $p_0 V_c < 0$ and $F < 0$ the elastic, dielectric and the ferroelectric torques favor different equilibrium states $\theta = 0$, $\theta = 0$ or π, and $\theta = \pi$, respectively. Since the dielectric torque dominates at very high voltages ($\eta \to \infty$) two (linear) stable equilibrium states are possible with $B = 0$ or $B \to \pi^2/2$, respectively. In the latter state (π-state) one has $\theta(z{=}0) \approx \pi$ at the cell center, while θ bends back to $\theta(z{=}\pm\pi/2) = 0$ near the boundaries.

For intermediate voltages the bifurcation diagrams are plotted as functions $B(\eta)$ in Fig.3 with the reduced voltage η

$$\eta = \frac{V - V_c}{V_c}\ . \tag{13}$$

Motivated by the amplitude equation [2] the numerical studies were done here for three distinct values of F_{11}/F_{22} belonging to the three regimes called I, II, and III, which describe the three possibilities of the Frederiks instability and the restabilization to be continuous or discontinuous. In regime I the bifurcation at $\eta = 0$ is supercritical while the restabilization at η_r is also continuous (inverted backward). This restabilization threshold is indeed reached, since after increasing first with increasing values of η, B then decreases back to $B = 0$. Somewhat above η_r there is an unstable solution between the restabilized ground state and the isolated π-state. On the other hand, in regimes II and III the branch that bifurcates from the ground state ($B = 0$) at $\eta = 0$ never comes back to $B = 0$, i.e. the restabilized ground state is generally not reached in experiments. Above η_r there is an unstable branch between the ground state and the π-state. In regime III the bifurcation at $\eta = 0$ is subcritical and there are two linear stable (solid lines) and one linear unstable (dashed) branch even below $\eta = 0$. The range of this hysteresis can be quite large, especially for small values of F_{11}/F_{22}.

It should be mentioned, however, that the transition from the restabilization scenario to the π-state scenario does not necessarily take place at the same parameters, where regime I switches to regime II. An example is shown in Fig.4, where near η_r also the validity range of the amplitude equation is rather restricted.

V. Model System

Generally it is impossible to get analytic solutions of the fully nonlinear problem, but near the transitions, for still small values of the order parameter (in the so-called weakly nonlinear regime), an equation for the amplitude of the linear mode $\theta(t, z) = A(t) \cos z$ with $A \propto \eta^{1/2}$ can be derived systematically. This amplitude equation describes the small-B region (where $B = A(t \to \infty)$) of Figs.3 very well [2]. However, in order to get an analytical expression for the complete bifurcation scenarios we propose a phenomenological model, which looks similar to an amplitude equation

$$\partial_t A = \eta\,(1 - \eta)\, A - g(\eta)\, A^3 - A^5. \tag{14}$$

For a suitable choice of the function $g(\eta)$ the steady state solutions of Eq.(14) reproduce the bifurcation topologies of Figs.3 qualitatively correct and can be used to investigate analytically the appropriate bifurcation schemes. There is the ground state $A = 0$ with the instability threshold at $\eta = 0$ and the restabilization at $\eta = 1$ (the normalized η_r), and the Frederiks-

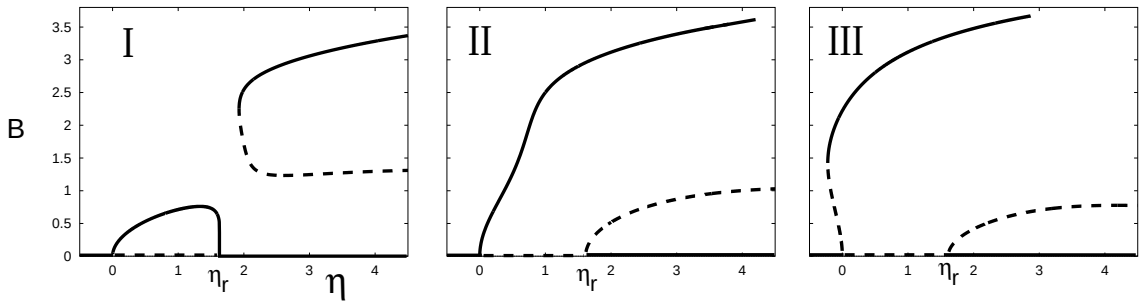

Fig.3 *The integrated director deformation B as function of the reduced voltage $\eta = (V - V_c)/V_c$ for $F = -0.2$ at 3 different values of F_{11}/F_{22} ($= 2.9, 1.5, 0.5$ from left to right).*

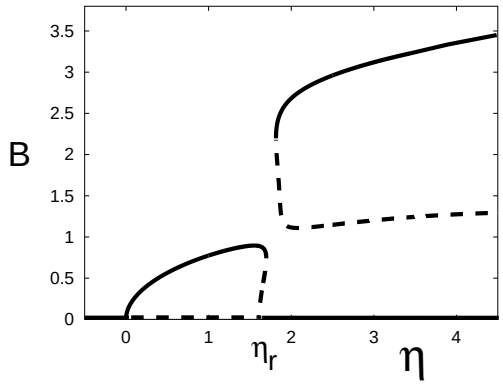

Fig.4 *A bifurcation scenario with discontinuous restabilization near* η_r *(*$F = -0.2, F_{11}/F_{22} = 2.75$*).*

unstable state with

$$A^2(\eta) = \frac{1}{2}\left[-g(\eta) \pm \sqrt{g^2(\eta) + 4\eta\,(1-\eta)}\right] \qquad (15)$$

with saddle nodes (vertical tangents) at $g^2(\eta)+4\,\eta\,(1-\eta) = 0$, where the stability of such a solution changes (from stable to unstable or vice versa).

With the simple ansatz

$$g(\eta) = S\,(C-\eta), \qquad (16)$$

where S and C are real constants, the restabilization and π-state scenarios can be reproduced. For $S > 0$ and $C > 1$, $0 < C < 1$, and $C < 0$ the topologies of regimes I, II, and III in Figs.3 are reobtained, respectively. Choosing S and fine-tuning C the position η_{SN} (and existence) of the saddle nodes can be fitted to the numerical results, since

$$\eta_{SN\,1,2} = \frac{S^2C - 2 \pm 2\sqrt{S^2C^2 - S^2C + 1}}{(S^2-4)} \qquad (17)$$

Fig.5 shows analytic plots of Eq.(15) for certain values of C and S, which look very similar to the numerical solutions in Fig. 3. The presented model system is not restricted to this special application of smectic C* liquid crystal films, but can be used for other systems showing restabilization.

VI. Electroconvection

In addition to the general Frederiks transition presented here, also electroconvection can occur, when an external electric field is applied to the film [1, 8]. While the Frederiks transition is homogeneous in x-direction ($q_c = 0$) electroconvection shows a pattern along x with a characteristic wavenumber $q_c \neq 0$. For a certain range of material parameters both instability types are possible and a competition between Frederiks with the electroconvective instability takes place. If a pure electroconvective pattern formation is searched, we suggest experiments with $F < -1/4$, since no Frederiks transition is possible there (cf. Fig.2). For DC voltages, in addition, all parameter values $F < 0$ will lead to an electroconvective transition, if the field is parallel to the polarization (upper left region of Fig.2). On the other hand all (big) positive values of F will prefer the Frederiks transition $q_c = 0$ (cf. [2] for details).

References

[1] S.Ried, H. Pleiner, W. Zimmermann, and H. R. Brand, in *24. Freiburger Arbeitstagung Flüssigkristalle* (Uni, Freiburg, 1995), p. P39.

[2] W. Zimmermann, S. Ried, H. Pleiner, and H. R. Brand, to appear in Europhys. Lett. (1996).

[3] H. R. Brand, P. E. Cladis, and P. L. Finn, Phys. Rev. **A31**, 361 (1985).

[4] S. W. Morris, J. R. de Bruyn, and A. May, Phys. Rev. Lett. **65**, 2378 (1990).

[5] E. Hoffmann and H. Stegemeyer, University of Paderborn, private communication, 1995.

[6] P. Pieranski, F. Brochard, and E. Guyon, J. Phys (Paris) **34**, 35 (1973).

[7] A. Saupe, Mol. Cryst. Liq. Cryst. **7**, 59 (1969).

[8] S. Ried, H. Pleiner, W. Zimmermann, and H. R. Brand, to appear in Phys. Rev. E (1996).

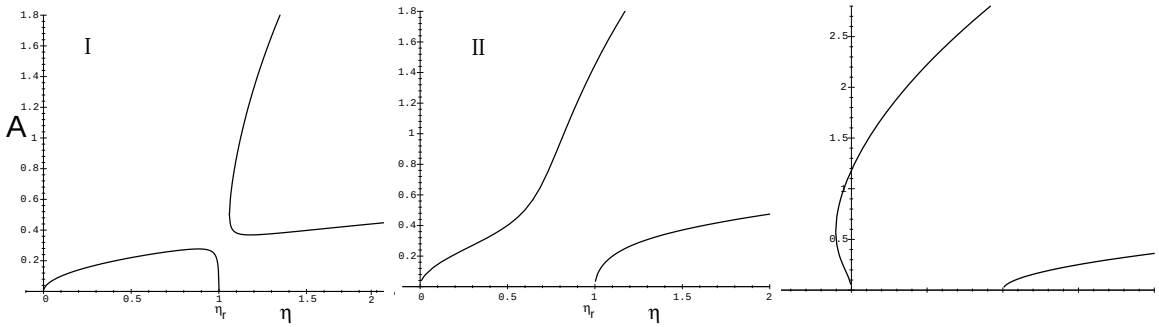

Fig.5 *The bifurcation scenarios of the model system Eq.(14) for some choices of the parameters* C *and* S *reproducing the regimes I, II, and III of Fig. 3.*